INTERNATIONAL JOURNAL OF OPTIMIZATION IN CIVIL ENGINEERING
Int. J. Optim. Civil Eng., 2019; 9(4):629-650

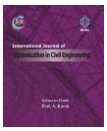

TOPOLOGY OPTIMIZATION OF PRETENSIONED CONCRETE BEAMS CONSIDERING MATERIAL NONLINEARITY

V. Shobeiri and B. Ahmadi-Nedushan[*, †]
Department of Civil Engineering, Yazd University, Yazd, Iran

ABSTRACT

In this paper, the bi-directional evolutionary structural optimization (BESO) method is used to find optimal layouts of 3D prestressed concrete beams. Considering the element sensitivity number as the design variable, the mathematical formulation of topology optimization is developed based on the ABAQUS finite element software package. The surface-to-surface contact with a small sliding between concrete and prestressing steels is assumed to accurately model the prestressing effects. The concrete constitutive model used is the concrete damaged plasticity (CDP) model in ABAQUS. The integration of the optimization algorithm and finite element analysis (FEA) tools is done by using the ABAQUS scripting interface. A pretensioned prestressed simply supported beam is modeled to show capabilities of the proposed method in finding optimal topologies of prestressed concrete beams. Many issues relating to topology optimization of prestressed concrete beams such as the effects of prestressing stress, geometrical discontinuities and height constraints on optimal designs and strut-and-tie models (STMs) are studied in the example. The results show that the proposed method can efficiently be used for layout optimization of prestressed concrete beams.

Keywords: topology optimization; strut-and-tie models; 3D pretensioned concrete; material nonlinearity.

Received:10 March 2019; Accepted: 12 July 2019

1. INTRODUCTION

Optimization can be defined as the act of obtaining the best result under given conditions. The goal of any optimization algorithm is either to minimize the effort required or to maximize the desired benefit [1]. In recent decades, optimization algorithms are used in civil engineering domain to perform various tasks such as prediction of material properties [2-3]

[*]Corresponding author: Department of Civil Engineering, Yazd University, Yazd, Iran
[†]E-mail address: behrooz.ahmadi@yazd.ac.ir (B. Ahmadi-Nedushan)

and a variety of civil engineering design applications [4-9]. Structural optimization is a very useful and challenging field that has received significant attention by researchers and practicing engineers. Structural optimization problems can be categorized as follows: (1) finding optimal size of structural members (size optimization); (2) obtaining the optimal form of the structure (shape optimization); and (3) achieving optimal size as well as finding connectivity between structural members (topology optimization) [10]. It has been recognized that topology optimization can be effectively used in early stages of design and that it significantly improves the structural performance compared to other types of structural optimization (e.g. size and shape optimization). Topology optimization for discrete structures, such as trusses and frames, is to search for the optimal connectivity of the bars. In topology optimization of continuum structures, the optimal designs are obtained by determining the best locations and geometries of cavities in the design domains.

Topology optimization provides much more freedom and options and provides the designers an effective tool for creating novel conceptual designs for continuum structures [11]. Researchers have used various optimization approaches such as Method of Moving Asymptotes (MMA) [12], integrated optimization approach based on the concept of isogeometric analysis and level set method [13], a combination of isogeometric analysis and level set method [14], a combination of isogeometric analysis and an implicit function based on Non-Uniform Rational B-Spline (NURBS) basis functions [15], a combination of the solid isotropic material with penalization (SIMP) and unstructured polygonal finite element analysis [16] and a convex linearization approach combining linear and reciprocal approximation functions [17] for solving problems dealing with static and dynamic loads.

Considering the increasing need to design lightweight structures with low cost and high performance, topology optimization may be considered as one of the most important tools in engineering applications in recent years [18]. The primary task of topology optimization is to find the best structural layout in a predefined design domain so that all the design constraints are met [17]. It has been recognized that topology optimization significantly improves the structural performance compared to other types of structural optimization (e.g. size and shape optimization) and has great potential for application in construction industry, particularly concrete structures for the determination of optimal strut-and-tie models and reinforcement layout designs [19-22].

It has been found that prestressing has introduced new approaches of construction and enabled new types of structures to be built [23-24]. Three of the most challenging and useful applications of the prestressing in recent years have been for large sea structures (such as harbors, fixed and floating platforms, and off-shore terminals), nuclear power stations and bridges. Several techniques for prestressing have been developed in recent decades. They are generally classified into two major categories, pretensioning and posttensioning. Pretensioning generally means that a compressive stress is put into a structure before it begins its working life [25]. It is well-known that concrete is strong in compression but weak in tension. The basic idea of prestressing concrete is to counteract these tensile stresses that are developed under external loads [26]. It is well-known that the prestressed concrete was patented by P.H Jackson in 1886. However, it was not until the late 1940s that prestressed concrete really began to develop. Eugene Freyssinet is regarded as the father of the prestressed concrete. His studies in the subject and the tests carried out by him in the early 1900s were pioneer in the field of prestressing concrete.

There are numerous research studies for the optimization of prestressed concrete structures. For example, Barakat et al. [27] proposed a multi-objective reliability-based optimization method for the design of prestressed girder beams. Ahsan et al. [28] employed a global optimization method for the cost optimum design of posttensioned I-girder bridge. Sirca and Adeli [29] suggested a nonlinear technique for the minimum cost optimization of prestressed I-girder bridge structures. Rana et al. [30] applied an evolutionary algorithm for the optimal cost design of prestressed concrete bridge structures. Aydin and Ayvaz [26] employed a hybrid genetic algorithm to determine the optimum number of spans and optimum cross-sectional properties of prestressed concrete bridges. Kaveh et al. [31] studied the cost optimum design of post-tensioned concrete bridges using the modified colliding bodies optimization algorithm. Liang et al. [32] proposed a performance-based optimization (PBO) method to generate optimal STMs of 2D prestressed concrete beams. Amir and Shakour [33] applied a density-based approach for topology optimization of 2D prestressed concrete beams. However, it can be found that none of these studies deals with topology optimization of 3D prestressed concrete beams in which prestressing steel, contact model between concrete and steel, and actual behavior of concrete under tension and compression are accurately modeled.

In this paper, the BESO method is extended for topology optimization of prestressed concrete beams considering material nonlinearity. A pretensioned simply supported beam is modeled using the ABAQUS finite element software to accurately model the effects of prestressing. The surface-to-surface contact with a small sliding between the concrete and prestressing steel is assumed. The concrete damaged plasticity model is used to model the nonlinear behavior of concrete. The height constraint, prestressing stress and geometrical discontinuity will be found to highly effect on the optimal layouts of prestressed concrete beams. Based on our best knowledge, this paper is the first study to find optimal topologies of 3D prestressed concrete beams in which prestressing steel, contact between concrete and steel, and material nonlinearity of both concrete and steel are all considered The results confirm the efficiency of the proposed method in finding optimal layouts of prestressed concrete beams.

2. PROBLEM FORMULATION

Some parts of a structural concrete member are not as effective in carrying loads as other parts [20]. Finding the efficient parts in a loaded concrete structure, the optimal layouts can effectively be generated. Therefore, the development of the optimal layouts in a concrete structure can simply be converted to a topology optimization problem [34]. The classical topology optimization can be stated as follows [35-38]:

$$\begin{aligned} &\textit{Minimize} && C = \mathbf{F}^{\mathrm{T}}\mathbf{U} \\ &\textit{Subject to:} && V^{*} - \sum_{i=1}^{N} V_i x_i = 0 \\ & && x_i = 1 \ \ or \ \ x_{min} \end{aligned} \tag{1}$$

The objective of the above equation is to minimize the mean compliance *C*. The design variable x_i indicates the presence (1) or absence ($x_{min} = 0.001$) of an element. This is consistent with the design variables of the soft-killed BESO method. In equation (1), N and V^* denote the total number of elements and the prescribed volume, and F and U represent the global force and displacement vectors respectively. In the BESO method considering nonlinearity, the structure is optimized by the discrete design variables which can be defined using the element sensitivity number α_i [11]:

$$\alpha_i = -p x_i^{p-1}(E_i^e + E_i^p) \tag{2}$$

where p is the penalty exponent, and E_i^e and E_i^p are respectively the elastic and plastic strain energies of element *i*. Using the obtained sensitivity numbers, the void elements are ranked alongside the solid elements in terms of their importance. The element additional and removal criterion can be described as follows:

$$\begin{cases} \textit{elements are removed:} & \textit{if } \hat{\alpha}_i \le \alpha^{th} \\ \textit{elements are added:} & \textit{if } \hat{\alpha}_i > \alpha^{th} \end{cases} \tag{3}$$

where α^{th} is the threshold of the sensitivity number which can be calculated based on the prescribed volume in each iteration (V^{k+1}):

$$V^{k+1} = V^k(1 \pm ER) \tag{4}$$

where V^k is the volume for the current iteration and *ER* is the evolutionary volume ratio. It should be noted that in this study a procedure similar to Ref. [34] is employed to obtain mesh-independent and checkerboard-free solutions. A performance index is also used to evaluate the measure of the efficiency of the iterative process [39]:

$$PI^k = \frac{C_0 V_0}{C_k V_k} \tag{5}$$

where PI^k is the performance index at iteration *k*. C_0 and V_0 are the compliance and volume of the initial structure respectively. Similarly, C_k and V_k are the compliance and volume of the current design at iteration *k* respectively. The performance index can also be used as a stopping criterion during the optimization process. In this study, the performance index smaller than unity is defined as the sopping criterion.

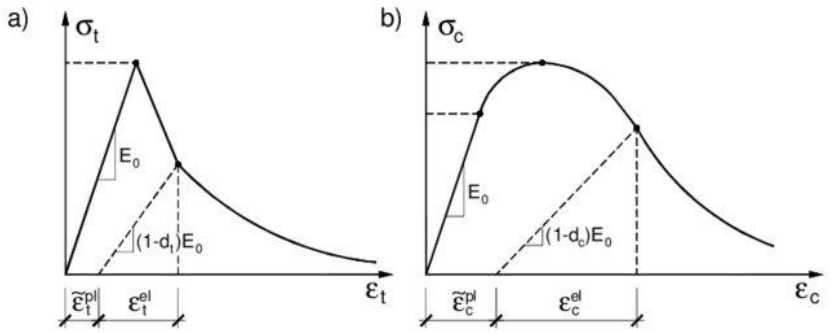

Figure 1. Response of concrete to uniaxial loading in: (a) tension; (b) compression

3. ABAQUS DAMAGED PLASTICITY MODEL

For nonlinear FE analysis, material model can play an essential role in predicting the strength of concrete. In this study, the damaged plasticity model in ABAQUS is used to model the tensile and compressive behavior of the concrete beam. The material model uses the isotropic damaged elasticity in association with isotropic tensile and compressive plasticity to represent the inelastic behavior of the concrete [40]. Both tensile cracking and compressive crushing are included in this model. Beyond the failure stress in tension, the formation of micro-cracks is represented macroscopically with a softening stress-strain response. The post-failure behaviour for direct straining is modeled by using the tension stiffening, which also allows for the effects of the reinforcement interaction with concrete [41].

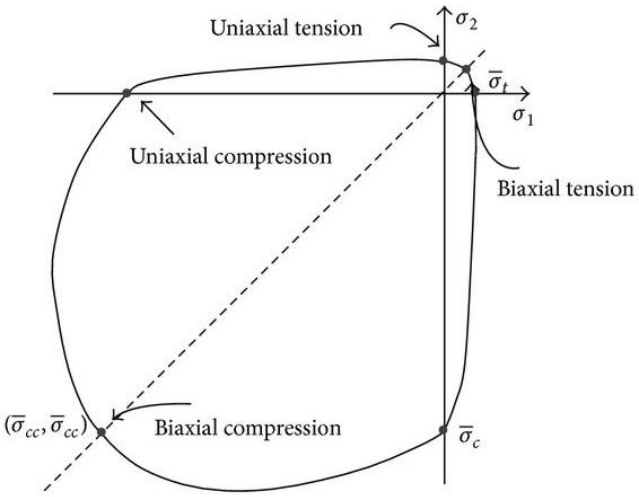

Figure 2. Yield surface of the concrete damaged plasticity model in a plane stress situation

The damaged plasticity model describes the uniaxial tensile and compressive response which is characterized by damaged plasticity as shown in Fig. 1. It is seen from Fig. 1.a that uniaxial tensile stress-strain response is linear elastic until the value of failure stress, and the

softening branch starts after violating this value. The uniaxial compressive response is linear elastic until the value of initial yield, followed by a hardening and a softening branch (see Fig. 1.b). It can also be seen from Fig. 1 that when the concrete member is unloaded from any point of strain softening branch of the stress-strain curve, the unloading response is weakened. The strain does not return to zero in an unloading situation, but some residual stresses remain present which is similar to the real behaviour of concrete [42].

In the CPD model, the elastic stiffness is characterized by two damage variables d_t and d_c, which are functions of plastic strains (ε_c^{pl} and ε_t^{pl}: equivalent plastic strain, $\dot{\varepsilon}_c^{pl}$ and $\dot{\varepsilon}_t^{pl}$: equivalent plastic strain rate). These two damage variables can take values from zero, representing the undamaged material, to one, which represents the total loss of the strength. Therefore, when E_0 is the initial undamaged elastic stiffness, the stress-strain relations under uniaxial tension and compression loading are respectively calculated as [40]:

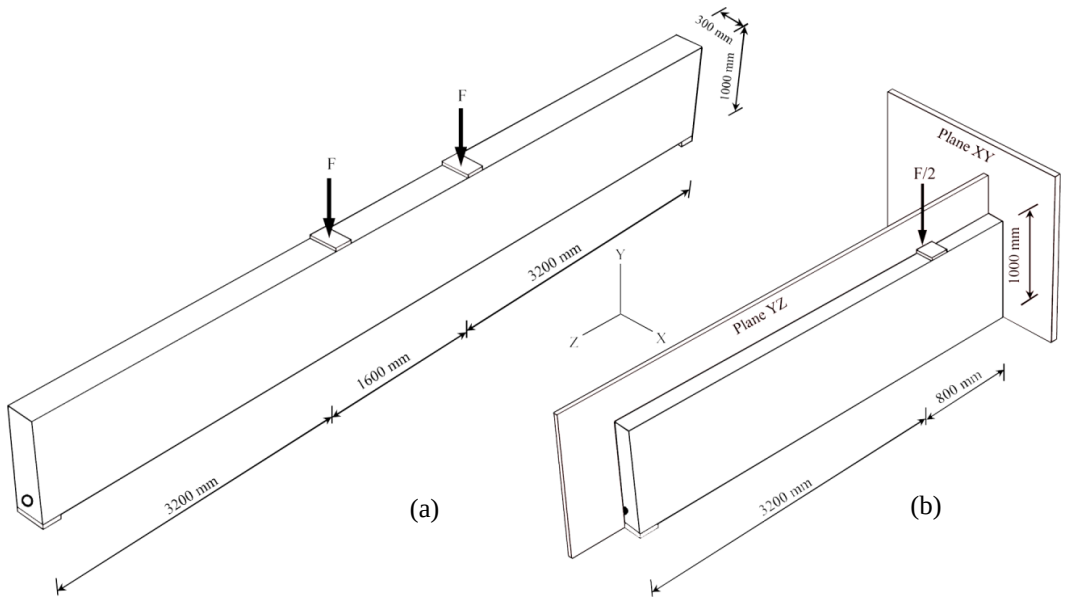

Figure 3. Simply supported prestressed concrete beam: (a) Full model; (b) Symmetric model

$$\begin{aligned} \sigma_t &= (1-d_t)E_0(\varepsilon_t - \varepsilon_t^{pl}) \\ \sigma_c &= (1-d_c)E_0(\varepsilon_c - \varepsilon_c^{pl}) \end{aligned} \tag{6}$$

Under uniaxial cyclic behaviour, the concrete damaged plasticity model assumes that the reduction of the elastic modulus is given in terms of a scalar degradation variable d_t as:

$$E = (1-d_0)E_0 \tag{7}$$

where d_0 is the stiffness degradation variable that is a function of the stress state and the uniaxial damage variables (d_t, d_c):

$$(1-d_0)=(1-s_t d_c)(1-s_c d_t) \tag{8}$$

where s_t and s_c are functions of the stress state. The stress-strain relations for the general three-dimensional multi-axial condition are given by scalar damage elasticity equation:

$$\bar{\sigma}=(1-d_0)\bar{\bar{D}}_0^{el}(\bar{\varepsilon}-\bar{\varepsilon}^{pl}) \tag{9}$$

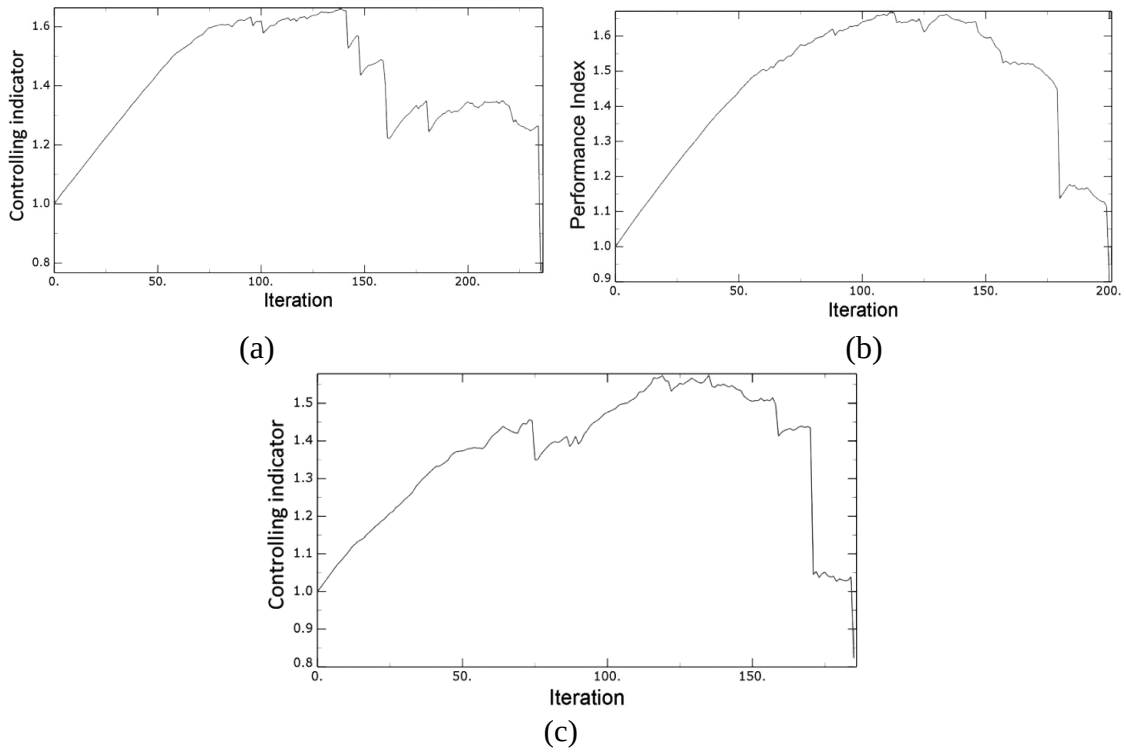

Figure 4. History of performance index: (a) f_p = 0; (b) f_p = 750 MPa; (c) f_p = 1500 MPa

where $\bar{\bar{D}}_0^{el}$ is the initial undamaged elasticity matrix and $\bar{\varepsilon}^{pl}$ is the strain at the end of the elastic part of the stress-strain curve. The linear elastic stress space is described by plasticity model based on a yield surface. The yield surface of the concrete damaged plasticity model is given in Fig. 2. It is worth noting that in a plane stress condition, the yield function presents a shape that is close to the real behavior of concrete. This shows that this material model can efficiently reflect the key characteristics of concrete.

4. LAYOUT OPTIMIZATION PROCEDURE

The main steps for the layout optimization of the prestressed concrete beams are given as follows:

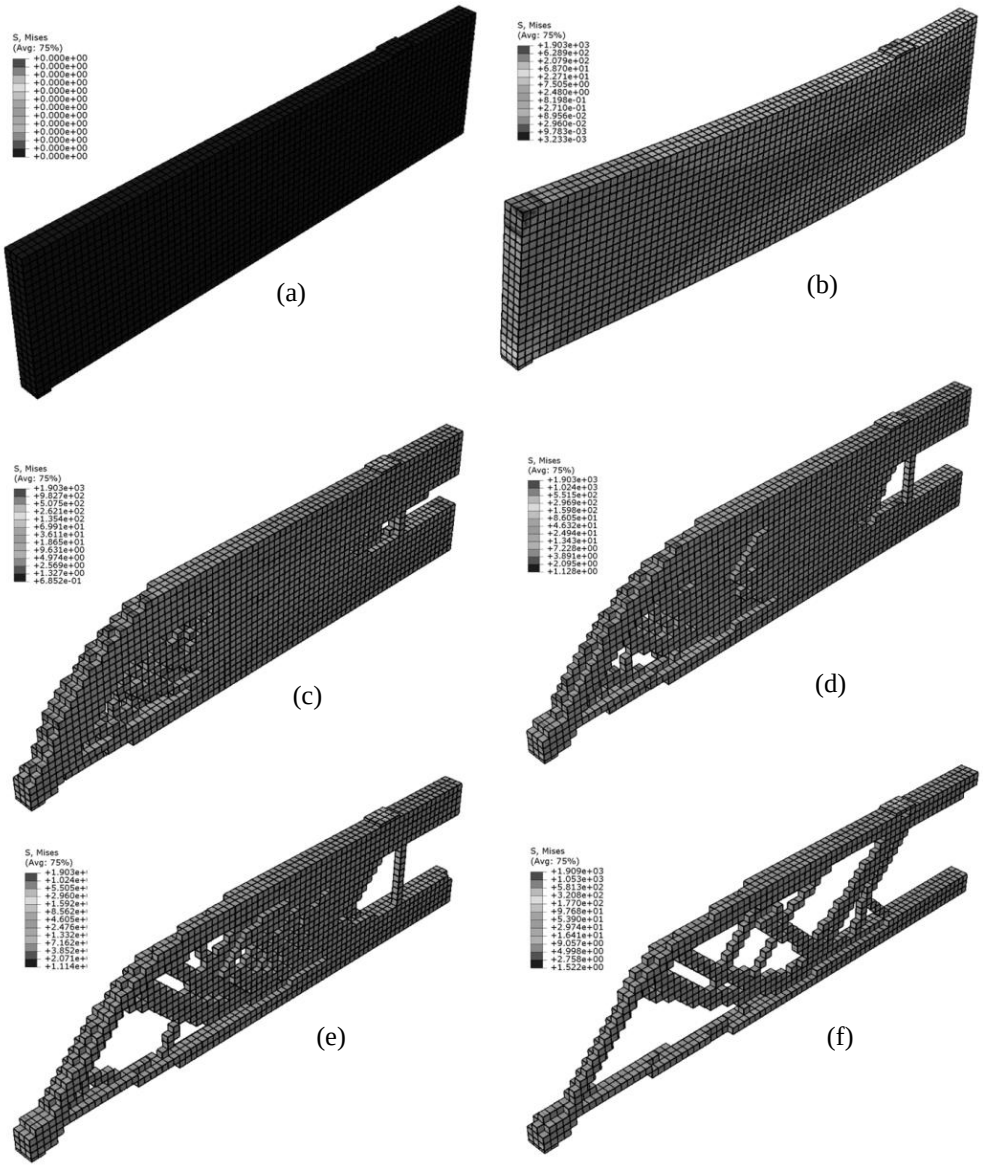

Figure 5. Optimization history of non-prestressed concrete beam (f_p = 0): (a) initial structure without loading; (b) initial structure with loading; (c) layout at iteration 30; (d) layout at iteration 60; (e) layout at iteration 90; (f) optimal layout (iteration 138)

1. Define 3D structural concrete, boundary conditions, external loading, bearing plates, prestressing steel, prestressing force, contact model, material properties and the finite element discretization. This step is fully carried out within the ABAQUS finite element software which provides a wide range of linear and nonlinear FEA meshing tools, material properties and contact modeling capabilities.

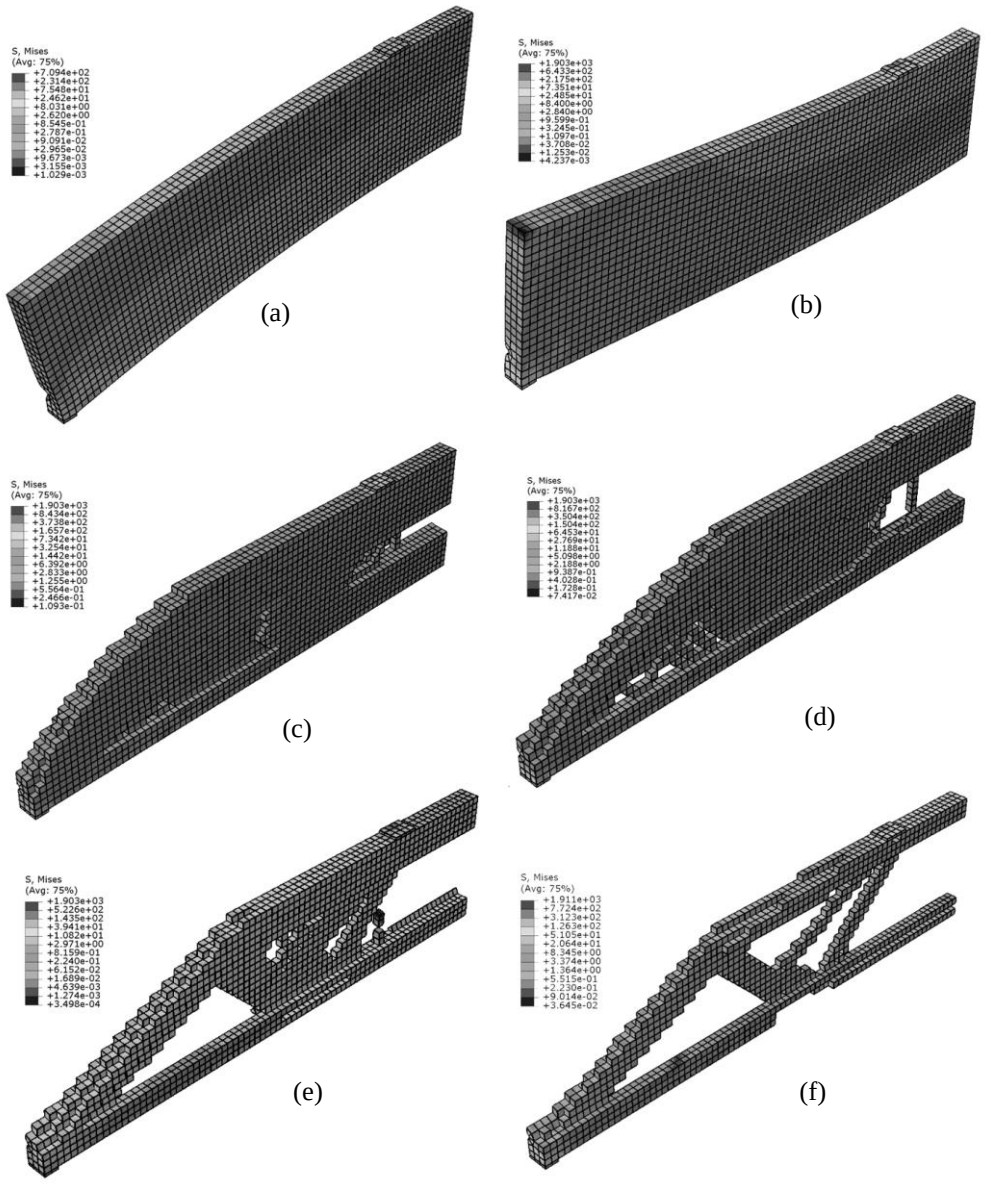

Figure 6. Optimization history of partially prestressed concrete beam (f_p = 750 MPa): (a) initial structure without loading; (b) initial structure with loading; (c) layout at iteration 30; (d) layout at iteration 60; (e) layout at iteration 90; (f) optimal layout (iteration 113)

2. Perform the nonlinear FEM analysis on the structural concrete and calculate the element sensitivity numbers according to Eq. (2).
3. Evaluate the efficiency of the resulting topology according to Eq. (5).
4. Compute the prescribed volume for the next iteration using Eq. (4).
5. Add or remove elements according to the value of their sensitivity numbers.

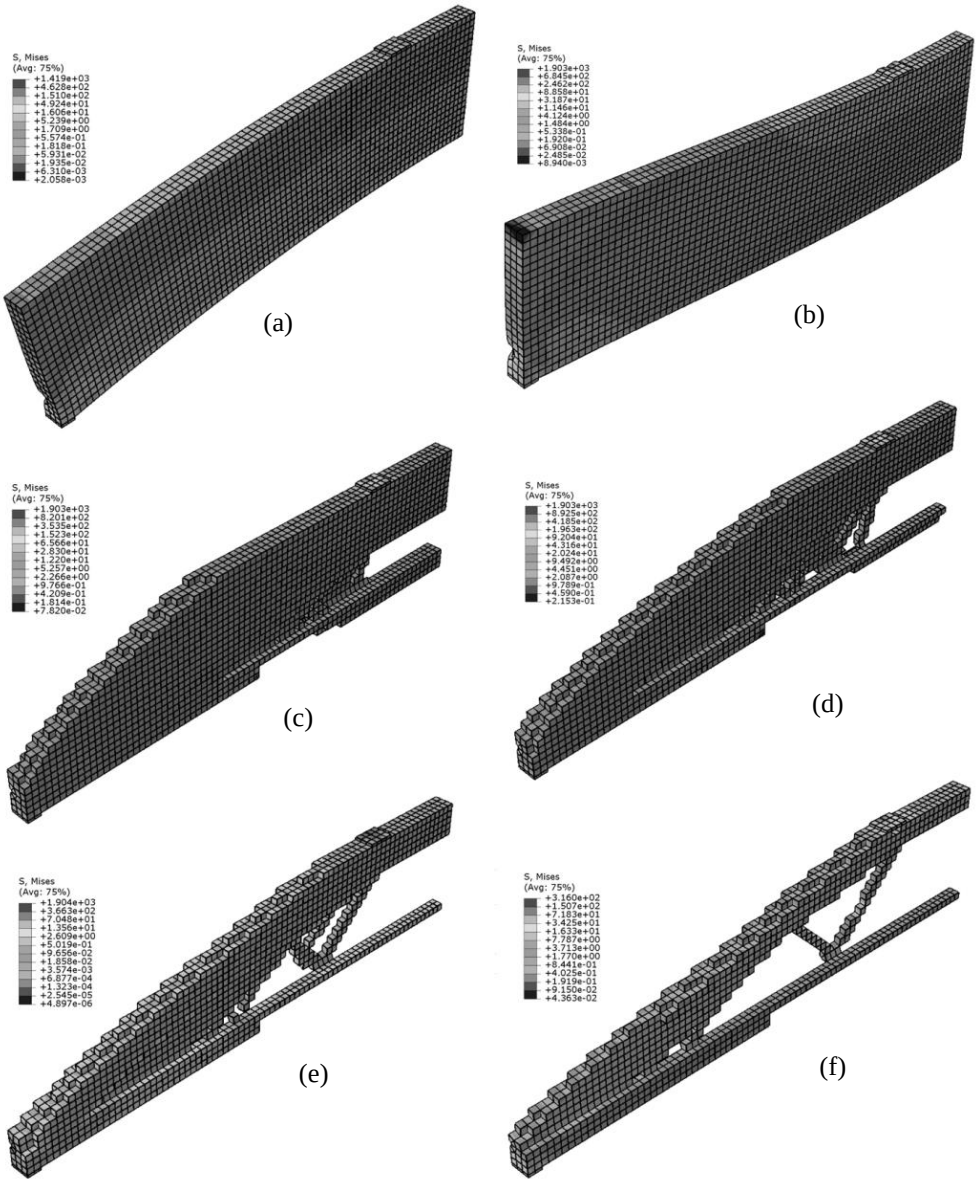

Figure 7. Optimization history of fully prestressed concrete beam (f_p = 1500 MPa): (a) initial structure without loading; (b) initial structure with loading; (c) layout at iteration 30; (d) layout at iteration 60; (e) layout at iteration 90; (f) optimal layout (iteration 136)

6. Repeat the steps of 2-5 until the performance index is less than unity.
7. Select the optimal layout that corresponds to the maximum performance index.

It should be noted that the ABAQUS scripting interface is used in this step to integrate the optimization procedure (BESO) and finite element tools.

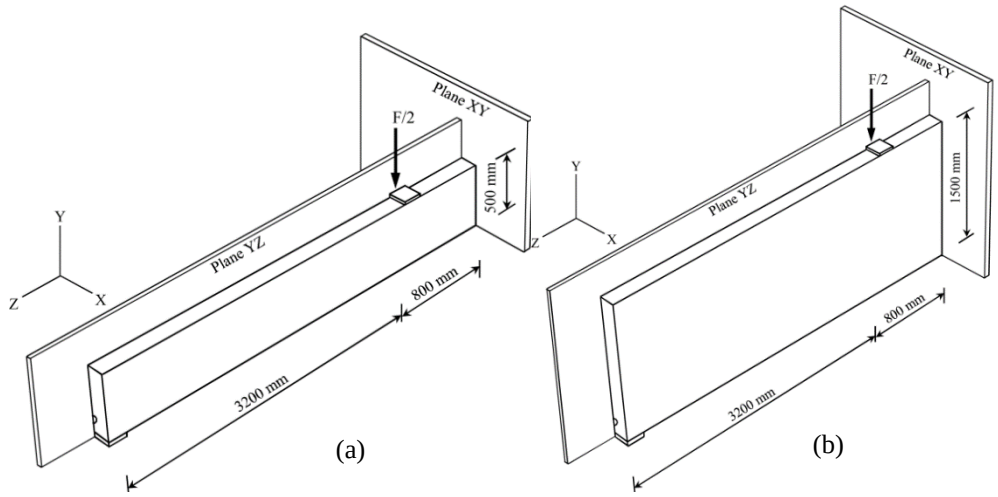

Figure 8. Prestressed concrete beam with different heights: (a) h = 500 mm; (b) h = 1500 mm

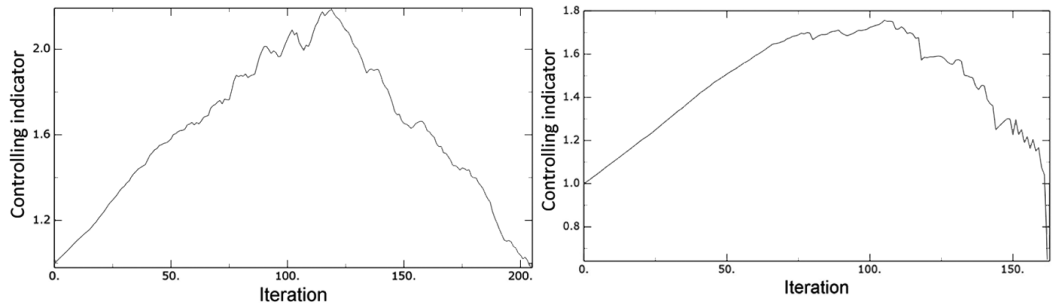

Figure 9. Performance index history with different heights: (a) h = 500 mm; (b) h = 1500 mm

5. NUMERICAL EXAMPLE

In this section, a pretensioned simply supported beam is presented to demonstrate the efficiency of the proposed method in finding optimal topologies of prestressed concrete beams. Several issues relating to the topology optimization of prestressed concrete beams such as the effects of prestressing stress, height constraint and geometrical discontinuities on optimal layouts are addressed in the example. Fig. 3.a shows the dimensions of the concrete beam with a rectangular cross section. The beam length to height size ratio is 8:1. The bottom right corner is a roller support and the bottom left corner is a fixed support. The width of the beam is assumed to be 300 mm. Two vertical forces of F = 500 kN are applied to the upper side of the structure. The prestressing steel with a diameter of 40 mm is placed at a distance of 150 mm from the bottom of the beam. It is assumed that bearing plates of 300×200 mm are used in the loaded points and supports. The ER = 1% is specified in the optimization process.

The concrete has the Young's modulus E = 31900 MPa and Poisson's ratio $\upsilon = 0.15$. The Young's modulus and Poisson's ratio of the prestressing steel are assumed to be E = 190 GPa and $\upsilon = 0.3$. The mass density of concrete and steel are considered to be 24 and 78 $\mathrm{KN\,m^{-3}}$. Due to symmetry, only a quarter of concrete beam and prestressing steel are modeled using 4960 8-node hexahedral elements and 320 wedge elements respectively (see Fig. 3.b). The full interaction between the elements of two materials is assumed. The surface-to-surface contact with small sliding between concrete and prestressing steel is considered in the analysis. An elasto-plastic model is employed for prestressing steels. The prestressing steel is meshed with the same size as that of the concrete to get more proper contact.

5.1 The effects of prestressing stress

The optimum value of prestressing force needs to be taken into account when analyzing and designing the prestressed concrete beams. To study the influence of prestressing force, the concrete beam is optimized with different values of prestressing stress: f_p = 0, 750 and 1500 MPa (namely nonprestressed, partially prestressed and fully prestressed). The performance index histories with various prestressing stress are shown in Fig. 4. It can be seen that the performance indices gradually increase in the optimization process and drop quickly after they approach their peak values. This can be referred to the breakdown of load transfer mechanism due to the element removal in a single iteration. The maximum performance index are respectively calculated as 1.64, 1.68 and 1.57 for the beam with prestressing stress of f_p = 0, 750 and 1500 MPa. It can be observed that the concrete structure with prestressing stress of f_p = 750 MPa has a higher performance index. This means that the concrete beam with partial prestressing has better performance than the nonprestressed and fully prestressed concrete beams.

The optimal topologies have resulted in material volume reductions of 25, 32 and 27 percent respectively for the structure with the prestressing stress of 0, 750 and 1500 MPa compared to the volume of the initial structure. The optimization histories and the optimal topologies with different values of prestressing stress are illustrated in Figs. 5-7. It can be seen that the value of prestressing stress highly affect optimal topologies, and that the optimal layouts varies with the change in the value of prestressing stress. It can also be observed that the number of bars in the final optimal topology considerably decreases with an increase in the value of prestressing stress. This shows that with an increase in prestressing stress, external loads transmit along a straighter load path. It can be concluded that the value of prestressing stress should be taken into account as an important factor for design of reinforcement layout in prestressed concrete beams.

5.2 The effects of height constraints

In practice, the design space of a concrete beam is often limited and significantly affects the optimal configurations of the structure. For instance, the height of a concrete bridge has to be limited in order to satisfy functional requirements [39]. Therefore, the designer should know how to select an initial design domain for finding the optimal structure in a given design space.

The effect of geometric restrictions such as height constraints on the optimal layouts of

prestressed concrete beams is investigated in this section. Fig. 8 illustrates the fully prestressed concrete beam (f_p = 1500 MPa) with various heights (h = 500 and 1500 mm). Fig. 9 shows the performance index history of the beam, and Figs. 10-11 depict the topology optimization histories and final optimal structures.

It can be seen from Fig. 9 that the performance index of the initial structure is equal to unity while the maximum performance indices for the structure with the height of 500 and 1500 mm are 1.76 and 2.19 respectively. As expected, the maximum performance index increases with an increase in the beam height.

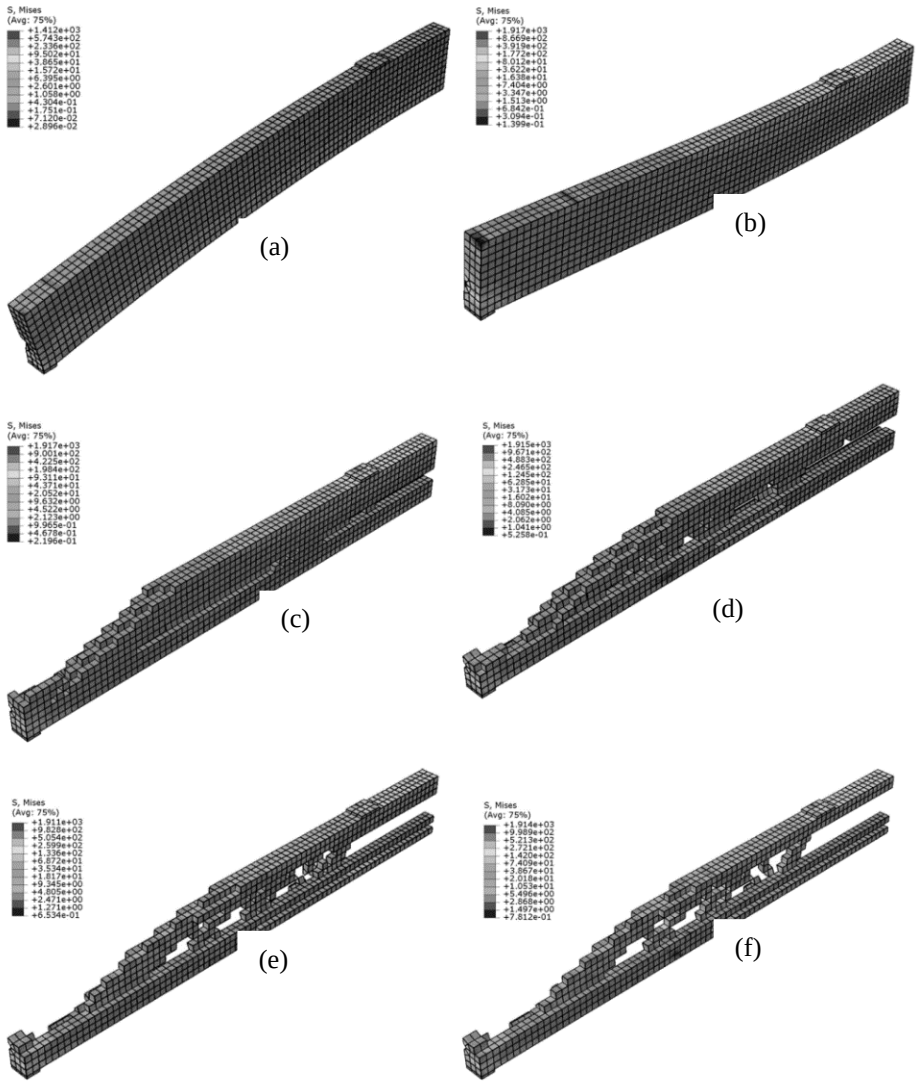

Figure 10. Optimization history of fully prestressed concrete beam (h = 500 mm): (a) initial structure without loading; (b) initial structure with loading; (c) layout at iteration 30; (d) layout at iteration 60; (e) layout at iteration 90; (f) optimal layout (iteration 106)

A comparison between Figs. 10 and 11 demonstrates that different optimal layouts are obtained for the same concrete beam with various height constraints. It can be confirmed that appropriate optimal topologies and reinforcement layout designs should be developed for the prestressed concrete beam with different heights.

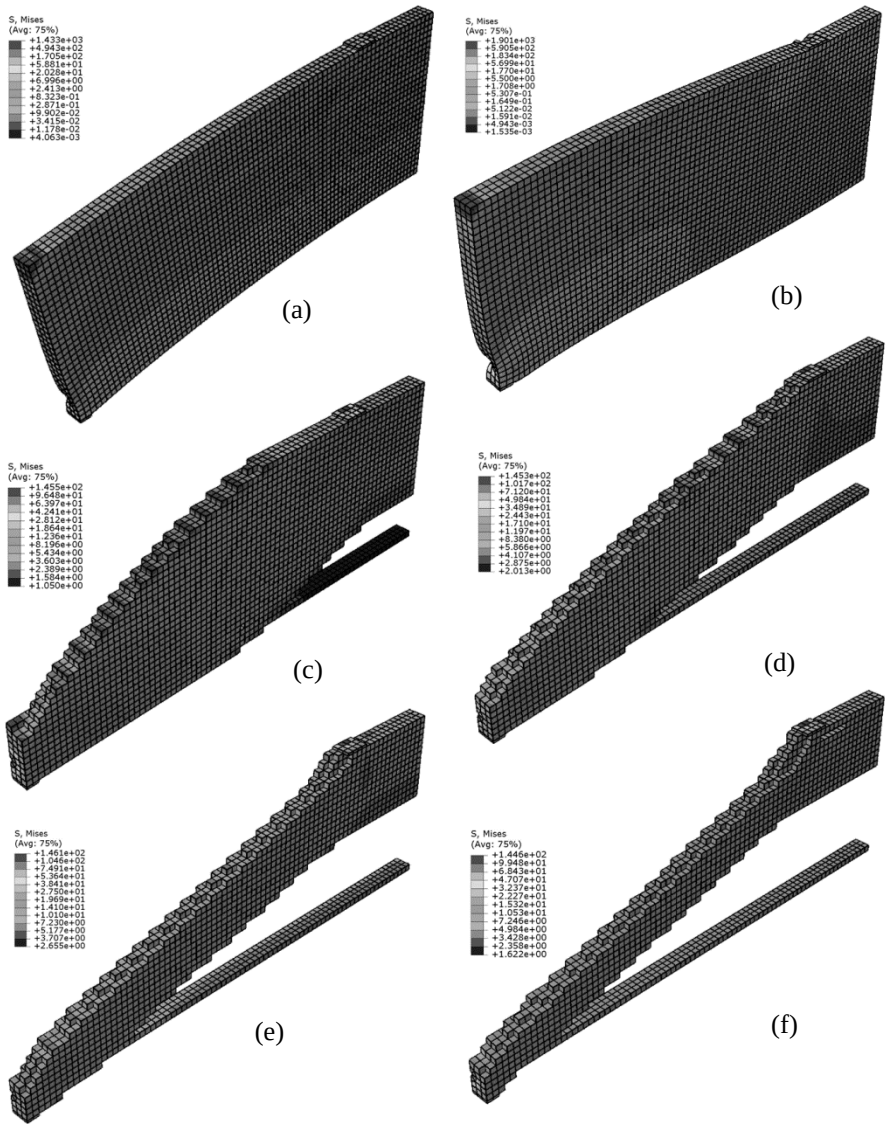

Figure 11. Optimization history of fully prestressed concrete beam (h =1500 mm): (a) initial structure without loading; (b) initial structure with loading; (c) layout at iteration 30; (d) layout at iteration 60; (e) layout at iteration 90; (f) optimal layout (iteration 120)

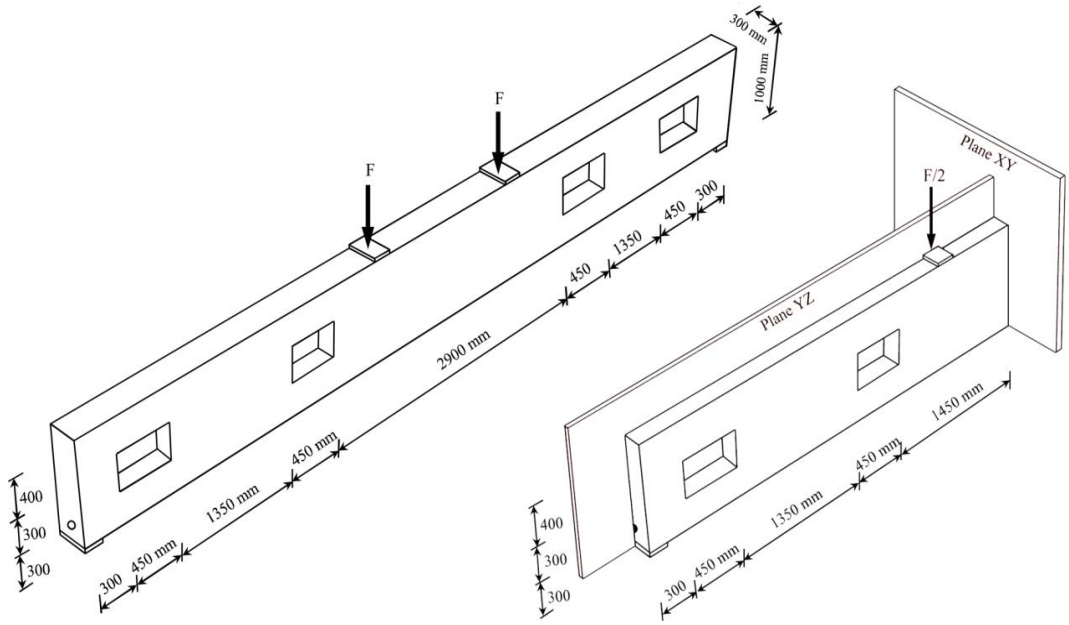

(a) (b)

Figure 12. Simply supported prestressed concrete beam with openings: (a) Full model; (b) Symmetric model

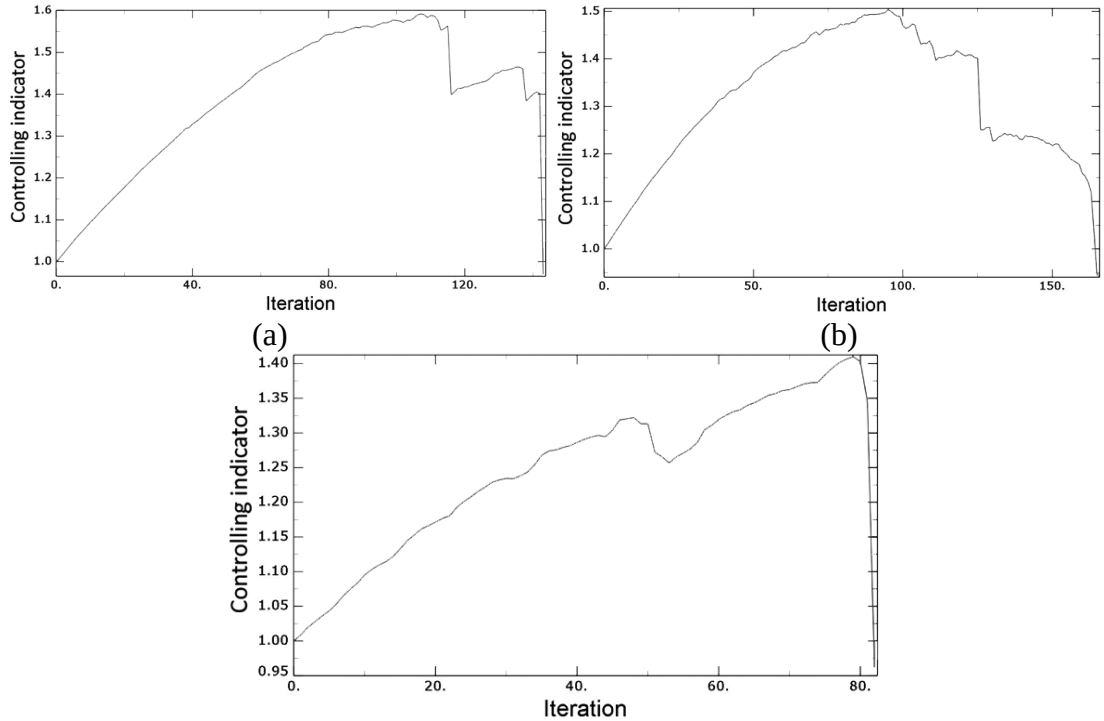

(a) (b)

(c)

Figure 13. Performance index history of beam with opening: (a) f_p = 0; (b) f_p = 750; (c) f_p = 1500 MPa

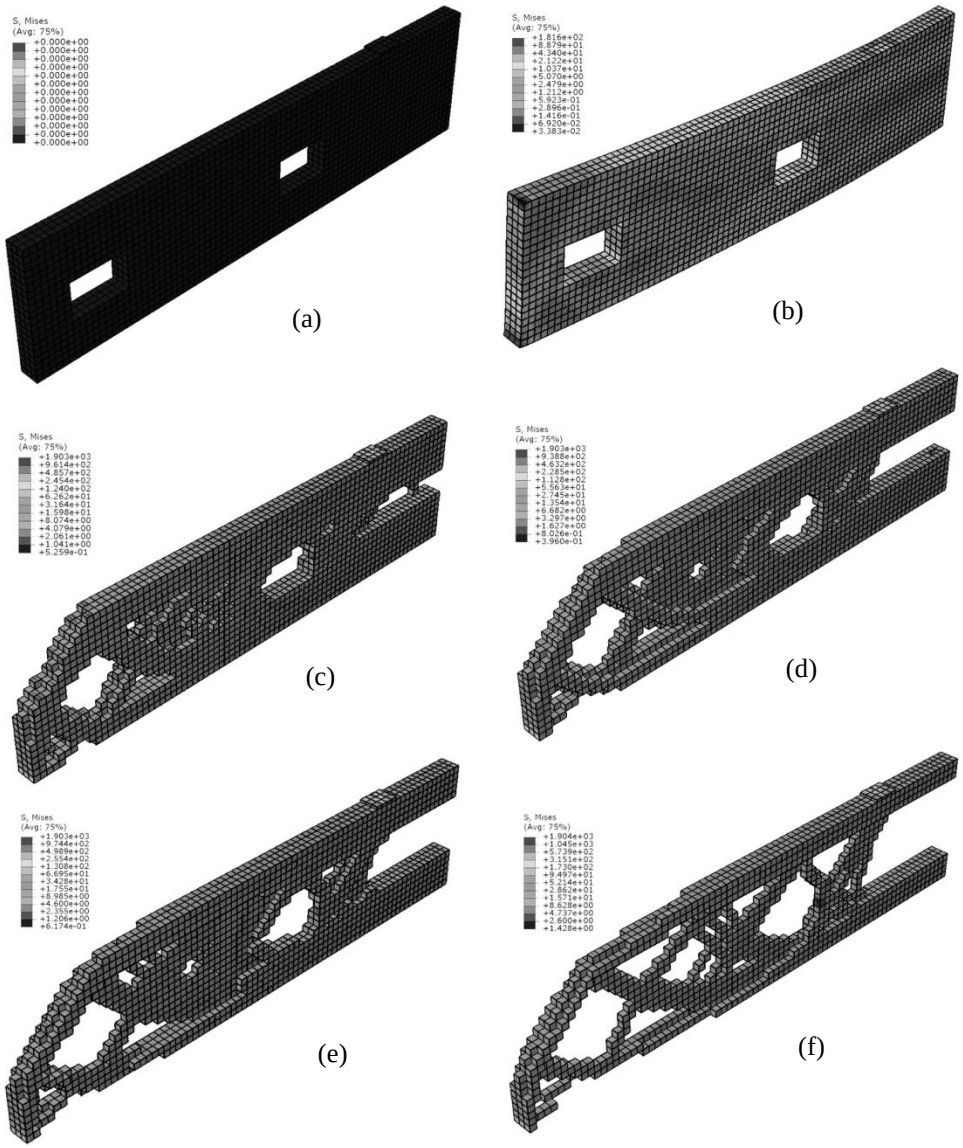

Figure 14. Optimization history of non-prestressed concrete beam (f_p = 0): (a) initial structure without loading; (b) initial structure with loading; (c) layout at iteration 20; (d) layout at iteration 40; (e) layout at iteration 60; (f) optimal layout (iteration 108)

5.3 The effects of openings

The purpose of this example is to examine the effect of geometrical discontinuities on the optimal layouts of prestressed concrete beams. Four openings are modeled on the vertical faces of the concrete beam as shown in Fig. 12.a. Due to symmetry, only a quarter of the concrete beam is modeled in the analysis (see Fig. 12.b). Fig. 13 shows the performance index histories of the concrete member under different values of prestressing stress (f_p = 0, 750 and 1500 MPa). The maximum performance indices for these cases are calculated as

1.59, 1.50 and 1.41 respectively. It is seen again that the maximum performance index decreases with an increase in the value of prestressing stress. The optimization histories and optimal topologies of the concrete beam with openings are depicted in Figs. 14-16.

A comparison between Figs. 14-16 and Figs. 5-7 reveals that the presence of geometrical discontinuities induces changes in inclined bars on the concrete beam. This is due to the fact that the load transfer path is cut by the openings. It can be observed that the presence of openings can significantly affect the optimal layouts in the prestressed concrete beams, and that the load-carrying system varies with the change in dimensions and size of openings.

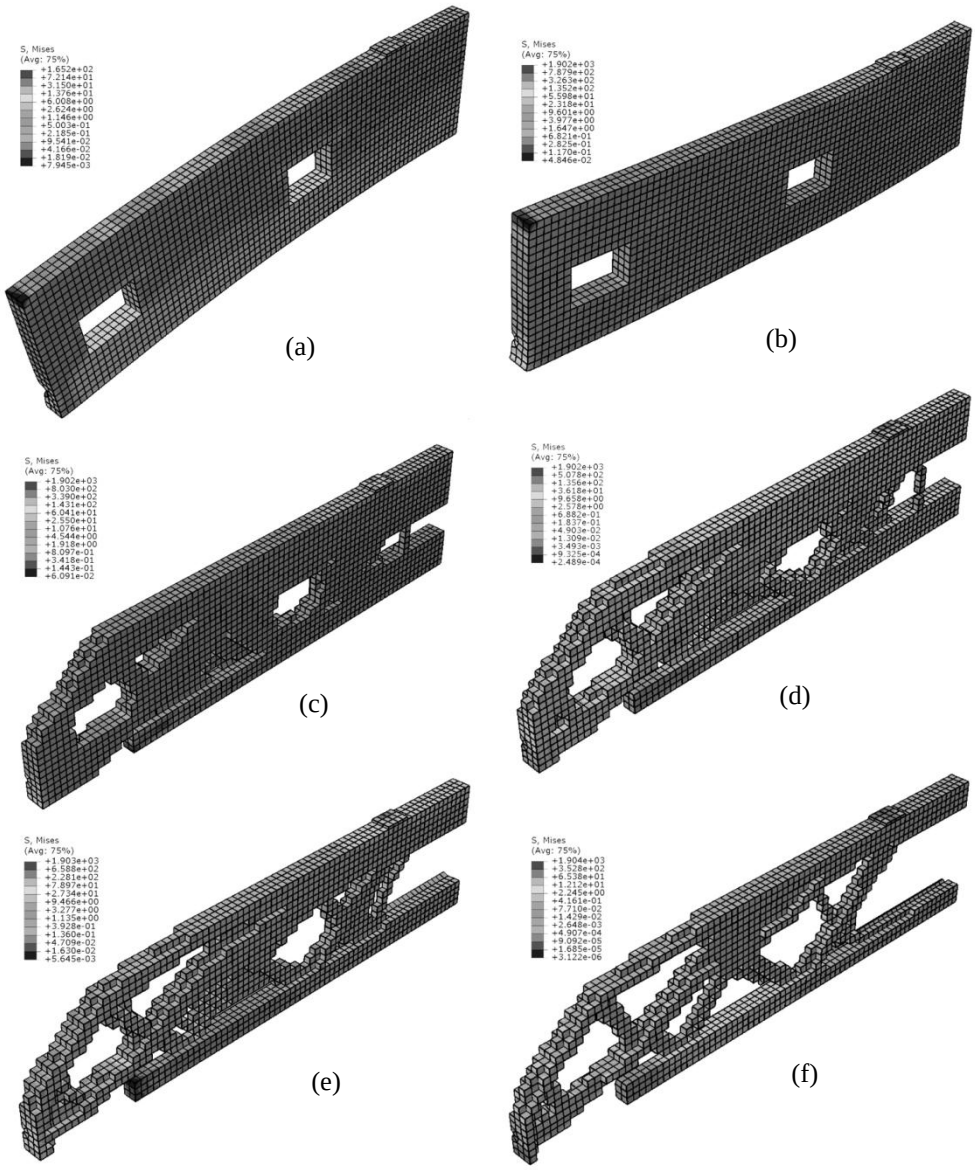

Figure 15. Optimization history of partially prestressed concrete beam (f_p = 750 MPa): (a) initial structure without loading; (b) initial structure with loading; (c) layout at iteration 20; (d) layout at iteration 40; (e) layout at iteration 60; (f) optimal layout (iteration 96)

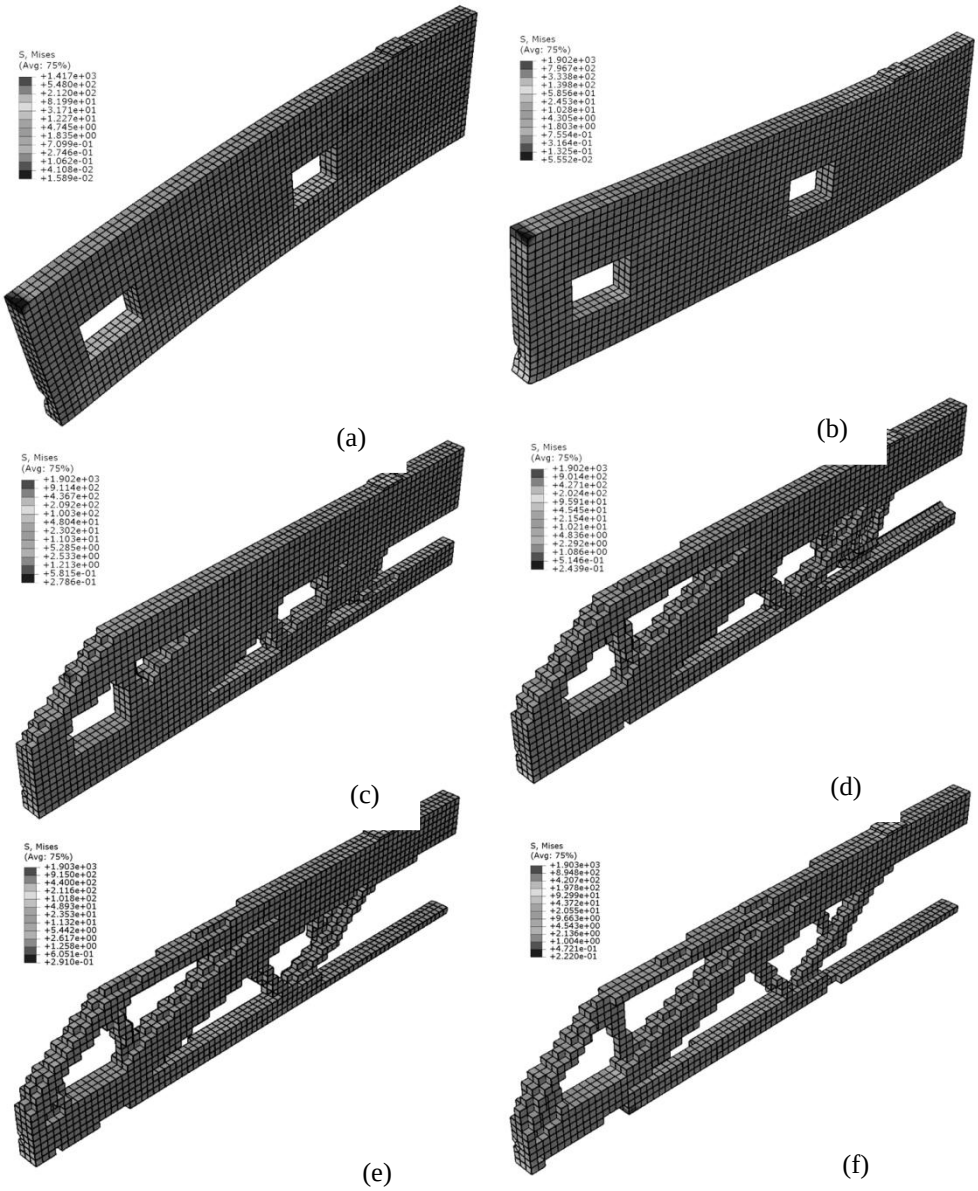

Figure 16. Optimization history of fully prestressed concrete beam (f_p = 1500 MPa): (a) initial structure without loading; (b) initial structure with loading; (c) layout at iteration 20; (d) layout at iteration 40; (e) layout at iteration 60; (f) optimal layout (iteration 80)

One of the most practical applications of topology optimization is to find optimal Strut-and-Tie Models (STMs) in concrete structures. A strut-and-tie model is an internal truss, comprising of concrete struts and steel ties that are connected at nodes to transform the applied loads through discontinuity regions to the supports [34]. It has been found that STMs can effectively be used for the flexural and shear design of structural concrete in disturbed regions [43-45]. The optimal topologies presented in Figs. 6 and 7 are idealized to the STMs shown in Fig. 17. It should be noted that the dashed and solid lines respectively

represent the concrete struts and steel ties. It can be found from a comparison between Figs. 17.a and 17.b that the value of prestressing stress considerably affects the optimal STMs in the prestressed concrete beam. It can also be seen that the applied loads are transferred from bearing plates to the supports through concrete struts tied by respectively three and two steel ties for the concrete structure with f_p = 750 and 1500 MPa. This shows that optimal STMs in the prestressed concrete beams considerably depend on the value of prestressing stress.

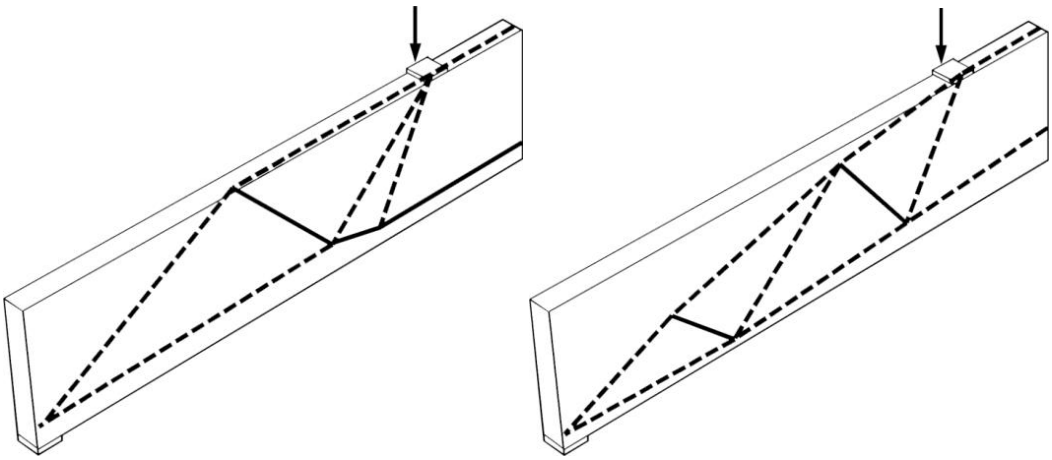

(a) (b)

Figure 17. Optimal strut-and-tie models obtained by present method: (a) partially-prestressing; (b) fully-prestressing

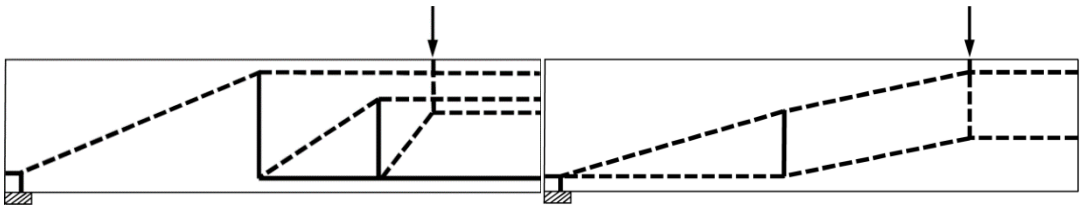

Figure 18. Optimal strut-and-tie models predicted by Schlaich et al. [30]: (a) partially-prestressing; (b) fully-prestressing

It has been recognized that conventional methods involving a trial-and-error iterative process based on the designer's intuition have no efficiency in finding appropriate STMs in prestressed concrete structures with complex geometry and loading conditions [39]. The STMs predicted by one such traditional method [46] for prestressed concrete beams are shown in Fig. 18. It is confirmed from a comparison between Figs. 17 and 18 that the STMs generated by the present method generally differ from those obtained by Ref. [46] and are in better agreement with the actual load-carrying systems in prestressed concrete beams [32]. This can be attributed to accurate modeling of the prestressing steels, contact between concrete and steel, and nonlinear behavior of concrete along with a efficient topology optimization method to find the load transfer mechanism in prestressed concrete beams.

6. CONCLUSION

This paper presents the BESO method for topology optimization of prestressed concrete beams considering material nonlinearity. The proposed method was implemented in the ABAQUS finite element software which provides a wide range of contact and nonlinear modelling tools. A pretensioned prestressed beam was presented to show the efficiency of the proposed framework in finding optimal layouts in prestressed concrete beams. Several issues relating to topology optimization of prestressed concrete beams such as prestressing stress, height constraint and geometrical discontinuity were studied in the example. The results show that the proposed method can effectively be used for the layout optimization of prestressed concrete beams.

REFERENCES

1. Rao SS. *Engineering Optimization: Theory and Practice*, John Wiley & Sons, 2009.
2. Ahmadi-Nedushan B. An optimized instance based learning algorithm for estimation of compressive strength of concrete, *Eng Applicat Artific Intelligen* 2012; **25**(5): 1073-81.
3. Ahmadi-Nedushan B. Prediction of elastic modulus of normal and high strength concrete using ANFIS and optimal nonlinear regression models, *Construct Build Mater* 2012; **36**: 665-73.
4. Biabani Hamedani K, Kalatjari VR. Structural system reliability-based optimization of truss structures using genetic algorithm, *Int J Optim Civil Eng* 2018; **8**(4): 565-86.
5. Kaveh A, Shokohi F, Ahmadi B. Optimal analysis and design of water distribution systems using tug of war optimization algorithm, *Int J Optim Civil Eng* 2017; **7**(2): 193-210.
6. Kaveh A, Zakian P. Stability based optimum design of concrete gravity dam using CSS, CBO and ECBO algorithms, *Int J Optim Civil Eng* 2015; **5**(4): 419-31.
7. Kaveh A, Zarandi MMM. Optimal design of steel-concrete composite I-girder bridges using three meta-heuristic algorithms, *Period Polytech Civil Eng* 2019; **63**(2): 317-37.
8. Varaee H, Ahmadi-Nedushan B. Minimum cost design of concrete slabs using particle swarm optimization with time varying acceleration coefficients, *World Appl Sci J* 2019; **13**(12): 2484-94.
9. Ahmadi-Nedushan B, Varaee H. Optimal design of reinforced concrete retaining walls using a swarm intelligence technique, *In The first International Conference on Soft Computing Technology in Civil, Structural and Environmental Engineering*, UK, 2009.
10. Kaveh A, Ilchi Ghazan M. *Meta-Heuristic Algorithms for Optimal Design of Real-Size Structures*, Springer, 2018.
11. Huang X, Xie M. *Evolutionary Topology Optimization of Continuum Structures: Methods and Applications*, John Wiley & Sons, 2010.
12. Yaghoobi N, Hassani B. Topological optimization of vibrating continuum structures for optimal natural eigenfrequency, *Int J Optim Civil Eng* 2017; **7**(1): 1-2.
13. Manafi I, Shojaee S. Solving multi constraints structural topology optimization problem with reformulation of level set method, *Int J Optim Civil Eng* 2018; **8**(2): 255-74.

14. Shojaee S, Mohamadianb M, Valizadeh N. Composition of isogeometric analysis with level set method for structural topology optimization, *International Int J Optim Civil Eng* 2012; **2**(1): 47-70.
15. Tavakkoli SM, Hassani B. Isogeometric topology optimization by using optimality criteria and implicit function, *Int J Optim Civil Eng* 2014; **4**(2): 151-63.
16. Akbarzaghi M, Ahmadi-Nedushan B. Improvement of pareto diagrams in topology optimization with unstructured polygonal finite element (In Persian), *J Ferdowsi Civil Eng* 2018; **31**(2): 89-102.
17. Alavi SA, Ahmadi-Nedushan B, Bondarabadi HR. Topology optimization of structures under transient loads, *Int J Optim Civil Eng* 2011; **1**: 155-66.
18. Shobeiri V. Topology optimization using bi-directional evolutionary structural optimization based on the element-free Galerkin method, *Eng Optim* 2016; **48**(3): 380-96.
19. Liang QQ, Uy B, Steven GP. Performance-based optimization for strut-tie modeling of structural concrete, *J Struct Eng* 2002; **128**(6): 815-23.
20. Kwak HG, Noh SH. Determination of strut-and-tie models using evolutionary structural optimization, *Eng Struct* 2006; **28**(10): 1440-9.
21. Johari M, Ahmadi-Nedushan B. Reliability-based topology optimization of bridge structures using first and second order reliability methods, *J Struct Construct Eng* 2017; **4**(1): 5-18.
22. Ozkal FM, Uysal H. Reinforcement detailing of a corbel via an integrated strut-and-tie modeling approach, *Comput Concr* 2017; **19**(5): 589-97.
23. Parol J, Al-Qazweeni J, Salam SA. Analysis of reinforced concrete corbel beams using strut and tie models, *Comput Concr* 2018; **21**(1): 95-102.
24. Menn C. *Prestressed Concrete Bridges*, Birkhäuser, 2012.
25. Kong FK, Evans RH. *Reinforced and Prestressed Concrete*, Springe, 2013.
26. Aydin Z, Ayvaz Y. Overall cost optimization of prestressed concrete bridge using genetic algorithm, *KSCE J Civil Eng* 2013; **17**(4): 769-76.
27. Barakat S, Bani-Hani K, Taha MQ. Multi-objective reliability-based optimization of prestressed concrete beams, *Struct Safe* 2004; **26**(3): 311-42.
28. Ahsan R, Rana S, Ghani SN. Cost optimum design of posttensioned I-girder bridge using global optimization algorithm, *J Struct Eng* 2011; **138**(2): 273-84.
29. Sirca Jr GF, Adeli H. Cost optimization of prestressed concrete bridges, *J Struct Eng* 2005; **131**(3): 380-8.
30. Rana S, Islam N, Ahsan R, Ghani SN. Application of evolutionary operation to the minimum cost design of continuous prestressed concrete bridge structure, *Eng Struct* 2013; **46**: 38-48.
31. Kaveh A, Maniat M, Naeini MA. Cost optimum design of post-tensioned concrete bridges using a modified colliding bodies optimization algorithm, *Adv Eng Softw* 2016; **98**: 12-22.
32. Liang QQ, Xie YM, Steven GP. Generating optimal strut-and-tie models in prestressed concrete beams by performance-based optimization, *ACI Struct J* 2001; **98**(2): 226-32.
33. Amir O, Shakour E. Simultaneous shape and topology optimization of prestressed concrete beams, *Struct Multidisc Optim* 2018; **57**(5): 1831-43.

34. Shobeiri V, Ahmadi-Nedushan B. Bi-directional evolutionary structural optimization for strut-and-tie modeling of three-dimensional structural concrete, *Eng Optim* 2017; **49**(12): 2055-78.
35. Kim H, Baker G. Topology optimization for reinforced concrete design, *In WCCM V Fifth World Congress on Computational Mechanics*, Vienna, Austria, 2002.
36. Rozvany GI. A critical review of established methods of structural topology optimization, *Struct Multidisc Optim* 2009; **37**(3): 217-37.
37. Shobeiri V. The topology optimization design for cracked structures, *Eng Analys Boundary Element* 2015; **58**: 26-38.
38. Dang HV, Lee D, Lee K. Single and multi-material topology optimization of CFRP composites to retrofit beam-column connection, *Comput Concre* 2017: **19**(4): 405-11.
39. Liang QQ. *Performance-based Optimization of Structures: Theory and applications*, CRC Press, 2014.
40. ABAQUS Manual, *ABAQUS 6.14 Analysis User's Manual*, Online Documentation Help: Dassault Systemes, 2014.
41. Nayal R, Rasheed HA. Tension stiffening model for concrete beams reinforced with steel and FRP bars, *J Mater Civil Eng* 2006; **18**(6): 831-41.
42. Hsu LS, Hsu CT. Complete stress-strain behavior of high-strength concrete under compression, *Magazine Concr Res* 1994; **46(**169): 301-12.
43. Hong SG, Lee SG, Hong S, Kang THK. Deformation-based strut-and-tie Model for flexural members subject to transverse loading, *Comput Concr* 2016; **18**(6): 1213-34.
44. Zhi Q, Guo Z, Xiao Q, Yuan F, Song J. Quasi-static test and strut-and-tie modeling of precast concrete shear walls with grouted lap-spliced connections, *Construct Build Mater* 2017; **150**: 190-203.
45. Ahmadi-Nedushan B, Kamalodini M, Baghadam N. Determining optimal strut-and-tie models for reinforced concrete disturbed region under multiple load using topology optimization, *Sharif J Civil Eng* 2017; **33**(2): 95-106.
46. Schlaich J, Schäfer K, Jennewein M. Toward a consistent design of structural concrete, *PCI J* 1987; **32**(3): 74-150.